

# Excitation of stellar p-modes by turbulent convection :

## 2. The Sun

Samadi R.<sup>1</sup>, Goupil M.-J.<sup>2</sup>, and Lebreton Y.<sup>2</sup>

<sup>1</sup> Observatoire de Paris. DESPA. CNRS UMR 8632. 92195 Meudon. France

<sup>2</sup> Observatoire de Paris. DASGAL. CNRS UMR 8633. 92195 Meudon. France

Received 17 October 2000 / Accepted 19 January 2001

**Abstract.** Acoustic power and oscillation amplitudes of radial oscillations computed for a solar model are compared with solar seismic observations. The oscillations are assumed to be stochastically excited by turbulence. The numerical computations are based upon a theoretical formulation of the power going into solar-like oscillation modes, as proposed by Samadi & Goupil (2001) in a companion paper. This formulation allows us to investigate several assumptions concerning properties of the stellar turbulence. We find that the entropy source plays a dominant role in the stochastic excitation compared with the Reynold stress source, in agreement with Goldreich et al. (1994). We consider several turbulent kinetic energy spectra suggested by different observations of the solar granulation. Differences between turbulent spectra manifest in large differences in the computed oscillation powers at high oscillation frequency. Two free parameters which are introduced in the description of the turbulence enter the expression for the acoustic power. These parameters are adjusted in order to fit to the solar observations of the surface velocity oscillations. The best fit is obtained with the kinetic energy spectrum deduced from the observations of the solar granulation by Nesis et al. (1993); the corresponding adjusted parameters are found to be compatible with the theoretical upper limit which can be set on these parameters. The adopted theoretical approach improves the agreement between solar seismic observations and numerical results.

**Key words.** convection - turbulence - Stars : oscillations - Sun: oscillations

### 1. Introduction

It is currently believed that oscillations of solar-like stars can be excited by the turbulent convection of their outer layers. The physical description of this stochastic excitation which yields the power transferred into the oscillations by the turbulence is not well known : the turbulent Reynolds stress was first identified (Goldreich & Keeley, 1977, hereafter GK) as the main source term. In the last decade, turbulent entropy fluctuations had been proposed as a possible additional source term (Stein & Nordlund, 1991; Balmforth, 1992; Goldreich et al., 1994).

In Paper I (Samadi & Goupil, 2001) we reconsider the excitation of stellar p-modes by turbulent convection. A new formulation following the GK approach and taking into account both Reynolds stress and entropy fluctuations contribution is proposed. In contrast with previous works, the present formulation is valid for any turbulent time spectrum and turbulent energy spectrum. The entropy source term was considered as the main source term by Goldreich et al. (1994, hereafter GMK) while

Balmforth (1992, hereafter B92) considered the corresponding contribution as negligible. However it was shown in Paper I that the entropy source term considered by GMK and B92 vanishes and a non-linear term involving the turbulent velocity field and the turbulent entropy represents the actual entropy contribution. Inherent to an empirical description of the stellar turbulence, our theoretical model for the acoustic power involves two free parameters, the parameter  $\lambda$  which is related to the rather arbitrary definition of eddy correlation time and the parameter  $\beta$  which relates the mixing length to the largest wavenumber in the inertial range.

Several space seismic experiments are currently planned : COROT (Baglin & The Corot Team, 1998), MONS (Kjeldsen & Bedding, 1998) and MOST (Matthews, 1998). These projects will provide very accurate seismic data such as oscillation amplitudes and damping rates for a large set of stellar targets. The oscillation powers deduced from these observations will provide valuable constraints on the current physical understanding of the excitation by turbulent convection. In the meantime, we need to validate and constrain our theoretical approach with current solar observations. This is the primary goal

of this paper. We first compute the oscillation power for a solar model (Sect. 2) using conventional assumptions for the turbulent components and compare it with observations. In Sect. 3 we investigate the influence of the atmosphere and of different turbulent components such as the time spectrum, the turbulent spectrum and the free parameters.

In Sect. 4, we discuss on the best treatment for the turbulent components and then calibrate the corresponding formulation on solar observations i.e. determine the free parameters in view of applications to other solar-like stars.

## 2. Oscillation power

### 2.1. Theoretical formulation and observations

The power going into each mode of frequency  $\omega_0$  is expressed as (see Paper I)

$$P_{\omega_0} = \Gamma_{\omega_0} E_{\omega_0} \quad (1)$$

where  $\Gamma_{\omega_0} = 2\eta$  is the linewidth of the mode,  $\eta$  is the damping rate and  $E_{\omega_0}$  is the averaged mode energy given by

$$E_{\omega_0} = \frac{1}{2} \langle |A|^2 \rangle I \omega_0^2, \quad (2)$$

where

$$I \equiv \int_0^M dm \xi^* \cdot \xi \quad (3)$$

is the mode inertia and  $\langle |A|^2 \rangle$  is the mean-square amplitude resulting from a balance between the excitation by the turbulent convection and damping processes. This amplitude can be expressed in a schematical form as

$$\langle A^2 \rangle \propto \eta^{-1} \int_0^M dm \rho_0 w^4 \left( \frac{\partial \xi_r}{\partial r} \right)^2 \mathcal{S}(\omega, m) \quad (4)$$

where  $\xi_r$  is the radial displacement eigenfunction,  $\rho_0$  the density,  $w$  the vertical rms velocity of the convective elements and  $\mathcal{S}$  the turbulent source function including both the Reynolds and the entropy fluctuation contributions. Detailed expressions for  $\langle A^2 \rangle$  and  $\mathcal{S}$  are given in Paper I. The source function involves the kinetic energy spectrum  $E(k)$ , the entropy energy spectrum  $E_s(k)$  and the time spectrum  $\chi_k(\omega)$ . The turbulent spectra in  $\mathcal{S}$  are integrated over all eddy wavenumbers  $k$ , and  $\mathcal{S}$  is in turn integrated in Eq.(4) over the stellar mass  $M$ .

The time spectrum  $\chi_k(\omega)$  measures the temporal coherence of eddies with given  $k$ . The linewidth of this function is related to the time correlation  $\tau_k$  associated with eddies with wavenumber  $k$ .  $\tau_k$  is related to  $k$  and the eddy velocity  $u_k$  by (see Eq. 97 of Paper I)

$$\tau_k = \lambda (k u_k)^{-1} \quad (5)$$

where the free parameter  $\lambda$  is introduced because the definition of the eddy correlation time  $\tau_k$  and the evaluation

of the eddy velocity are somewhat arbitrary. The eddy velocity  $u_k$  is given by Eq.(98) of Paper I. Several different time spectra are investigated later in this paper. In addition, we evaluate effect of changes in the parameter  $\lambda$ , which is usually set to one, for instance in B92.

The kinetic energy spectrum  $E(k)$  describes the energy carried by the turbulent eddies. In a highly turbulent medium, such as in the outer stellar convection zone, it is expected from turbulence theory that such a spectrum exhibits an inertial range where the energy carried by the eddies with wavenumber  $k$  decreases as  $k^{-5/3}$  in the Oboukhov-Kolmogorov theory. The wavenumber  $k_0$  at which the turbulent cascade begins is not well determined. This quantity has been related in Paper I to the mixing length  $\Lambda$  as

$$k_0 = \frac{2\pi}{\beta \Lambda}, \quad (6)$$

where  $\beta$  is a free parameter which has been introduced in order to gauge the arbitrary nature of such a relation. The injection region lies in the  $k \leq k_0$  range. Here we investigate several turbulent kinetic energy spectra exhibiting different forms in the injection region.

The mean-square amplitude is inversely proportional to the damping rate (e.g. Balmforth, 1992) and consequently the acoustic noise generation rate (or acoustic power)  $P_{\omega_0}$  is independent of  $\eta$ . Thus comparing the estimated acoustic noise generation rates with observations avoids the additional uncertainties in the modeling of the damping rates (GMK) but requires accurate linewidth measurements and model computations.

The mean-square surface velocity of a mode is given by the relation (see Paper I)

$$v_s^2(\omega_0) = \omega_0^2 \xi^2(r_s) \frac{1}{2} \langle |A|^2 \rangle = \xi^2(r_s) \frac{P_{\omega_0}}{2\eta I} \quad (7)$$

where  $r_s$  is the radius of the layer seen by the instrument. Observations of  $v_s$  performed by Libbrecht (1988) are plotted in Fig. 1 with accompanying error bars. The surface velocity amplitude  $v_s$  steeply increases with frequency at low frequencies, presents a maximum value around  $\nu \simeq 3.2$  mHz and undergoes a steep decline at high frequency. In Sect. 4 we make use of these three characteristics to constrain the turbulent ingredients and the free parameters entering the theory of the excitation process.

### 2.2. Oscillation power in the solar case

The solar model we consider has been calculated with the CESAM code (Morel, 1997) and appropriate input physics, described in details in Lebreton et al. (1999). In particular, convection is described according to the classical mixing-length theory (Böhm - Vitense, 1958, hereafter MLT) with a mixing-length  $\Lambda = \alpha_c H_p$ , where  $H_p$  is the pressure scale height and  $\alpha_c$  is the mixing-length parameter. The external boundary conditions are obtained through a  $T(\tau)$  law derived from ATLAS9 model atmospheres (Kurucz, 1991). The solar metal to hydrogen mass

ratio  $(Z/X)_{\odot} = 0.0245$  comes from Grevesse & Noels (1993). The calibration of the solar model, in luminosity ( $L_{\odot} = 3.846 \cdot 10^{33}$  erg/s) and radius ( $R_{\odot} = 6.9599 \cdot 10^{10}$  cm) for an age of 4.6 Gyr, fixes the initial helium content  $Y = 0.2682$ , metallicity  $Z = 0.0175$  and the MLT parameter  $\alpha_c = 1.785$ .

The estimated cut-off frequency is about  $\nu_c \simeq 5.32$  mHz. The oscillation eigenfunctions are obtained with the adiabatic pulsation FILOU code of Tran Minh & Leon (1995).

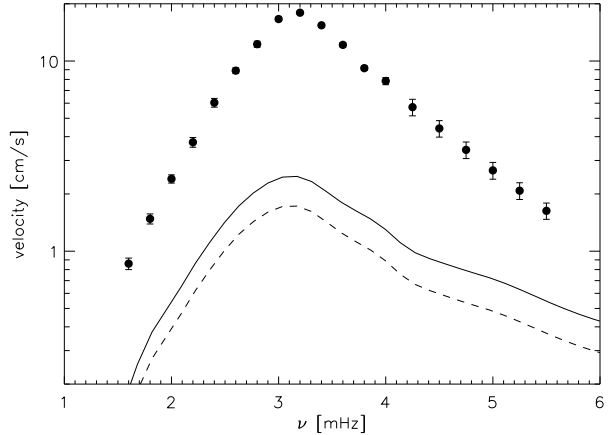
We evaluate the root mean-square surface velocity  $v_s$  in Eq.(7) where the oscillation power  $P_{\omega_0}$  is computed according to Eqs(1, 2, 4) and  $\eta$  is given by solar observations of Libbrecht (1988). These solar observations sample the solar atmosphere at the optical depth  $\tau_{5000} \simeq 0.05$ . In our solar model this optical depth is localized approximately at 140 km above the solar photosphere and  $v_s$  is thus computed at this depth.

Fig. 1 shows the resulting values of  $v_s$  assuming the Kolmogorov spectrum as defined in Eq.(8).

As in GMK and B92, it is assumed that the entropy spectrum exhibits the same behavior than the kinetic energy spectrum. Thus the entropy energy spectrum  $E_s(k)$  considered in the computation is at this stage simply proportional to the kinetic energy spectrum  $E(k)$  (Eq. 107 of Paper I). The parameter  $\lambda$  is first set to one and the parameter  $\beta$  is set to 1.9, according to the theoretical estimate obtained in Paper I. The anisotropic factor  $\Phi$  involved in the formulation may be considered as a free parameter. However in order to be consistent with Bohm-Vitense's MLT considered here, we set  $\Phi = 2$  in the present work.  $\Phi$  affects the  $\nu$  dependence of the power in a similar way as  $\lambda$  and  $\beta$ . Changing its value is therefore equivalent to change values of  $\lambda$  and  $\beta$ , which will be adjusted later (section 4).

At low frequencies,  $v_s$  increases because the inertia of the modes decreases with frequency and because the derivatives of the displacement eigenfunctions increase with frequency (see GMK). At high frequency,  $v_s$  decreases because the depth of the excitation region and the efficiency of the excitation decrease with frequency. This can be explained as follows: let  $\tau_k$  be the characteristic lifetime of an eddy of wavenumber  $k$ . The major contribution to mode excitation comes from the eddies with  $\tau_k \omega_0 \lesssim 1$  (Goldreich & Kumar, 1990, Paper I). When  $\omega_0$  increases, the region where  $\tau_k \omega_0 \lesssim 1$  becomes thinner and is confined at the top of the convection zone. Furthermore, contributive eddies have smaller size and are less energetic. Thus  $P_{\omega_0}$  becomes smaller as  $\omega_0$  increases.

Including only the Reynolds stress leads to amplitudes much smaller than those observed. The contribution of the entropy source term is found to be larger than the Reynolds stress contribution and increases the amplitudes. This result is in agreement with the conclusion of GMK and with the simulations of Stein & Nordlund (1991). However, some discrepancy still remains between the theoretical estimates and the observations. In particular the theoretical absolute amplitudes remain much smaller than



**Fig. 1.** Root-mean-square velocity  $v_s(\omega_0)$ : dots with accompanying error bars represent the solar measurements of Libbrecht (1988). The continuous curve shows velocity amplitudes computed according to Eq.(7) using both the Reynolds and the entropy contributions and the dashed curve using only the Reynolds stress contribution. A Kolmogorov energy spectrum is assumed. Damping rates are deduced from Libbrecht (1988) and we assumed  $\lambda = 1$  and  $\beta = 1.9$ .

the observed ones and large differences are observed at high frequency in terms of frequency dependence between the amplitudes computed using the Kolmogorov spectrum and the observations. Also, the maximum amplitude peaks at a frequency which is smaller by about 0.1 mHz, compared to the observed position of the maximum.

### 3. Impact of different assumptions

The above calculations were performed considering standard assumptions for the turbulent spectra and the free parameter  $\lambda$ . We now investigate effects of changing the turbulent properties, the free parameters  $\lambda$  and  $\beta$ , the treatment of the atmosphere and of the depth in the atmosphere at which the expected surface velocity  $v_s$  is computed.

#### 3.1. Turbulent kinetic energy spectrum

In Sect. 2 we considered the Kolmogorov Spectrum (KS hereafter)

$$E(K) = \frac{u_0^2}{k_0} K^{-5/3} \text{ for } K > 1 \quad (8)$$

where  $K \equiv k/k_0$ ,  $k_0 = 2\pi/(\beta\Lambda)$  and  $u_0^2$  is proportional to the mean square turbulent velocity (see Paper I).

Observations of solar granulation show a change of slope of the kinetic energy spectrum between the inertial range where the spectrum obeys the Kolmogorov law and the large scale range (small wavenumbers  $k$ ) corresponding to the energy injection region.

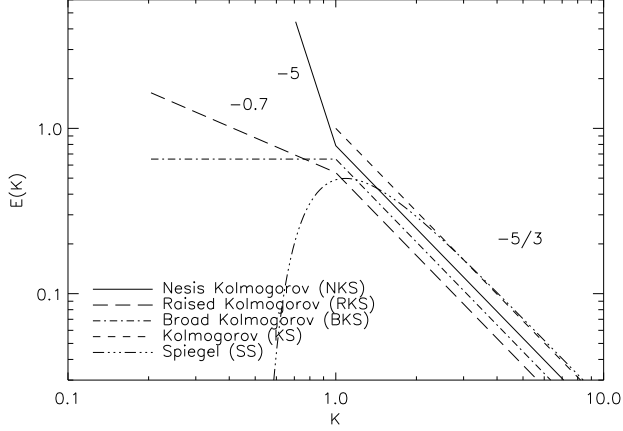


**Fig. 2.** The RKS, KS, SS, BKS and NKS versus the normalized wavenumber  $K$ . The NKS has been shifted up in order to distinguish it from the BKS for  $K > 1$

In order to take large scale eddies into account, we consider first the Spiegel spectrum (SS hereafter) for comparison with B92 and Houdek (1996).

$$E(K) = 18 \frac{u_0^2}{k_0} (2K)^{-5/3} J(2K) \text{ for } K > 0.5 \quad (9)$$

with

$$J(K) = \left[ 1 - K^{-8/3} - \frac{4}{7}(1 - K^{-14/3}) \right]^2. \quad (10)$$

This spectrum takes into account the non-linear interaction between turbulent modes of low wavenumber (Spiegel, 1962; Stein, 1967) and is built for very large Rayleigh numbers.

In order to match the high-resolution observations of the solar granulation by Roudier & Muller (1986), Musielak et al. (1994) has proposed the ‘‘Raised Kolmogorov Spectrum’’ (RKS hereafter)

$$E(K) = \begin{cases} 0.54 \frac{u_0^2}{k_0} K^{-5/3} & \text{for } K > 1 \\ 0.54 \frac{u_0^2}{k_0} K^{-0.7} & \text{for } 0.2 < K < 1 \end{cases} \quad (11)$$

and as a possible alternative the ‘‘Broad Kolmogorov Spectrum’’ (BKS hereafter)

$$E(K) = \begin{cases} 0.652 \frac{u_0^2}{k_0} K^{-5/3} & \text{for } K > 1 \\ 0.652 \frac{u_0^2}{k_0} & \text{for } 0.2 < K < 1. \end{cases} \quad (12)$$

We also consider the ‘‘Nesis Kolmogorov Spectrum’’ (NKS, hereafter)

$$E(K) = \begin{cases} 0.655 \frac{u_0^2}{k_0} K^{-5/3} & \text{for } K > 1 \\ 0.655 \frac{u_0^2}{k_0} K^{-5} & \text{for } 0.7 < K < 1 \end{cases} \quad (13)$$

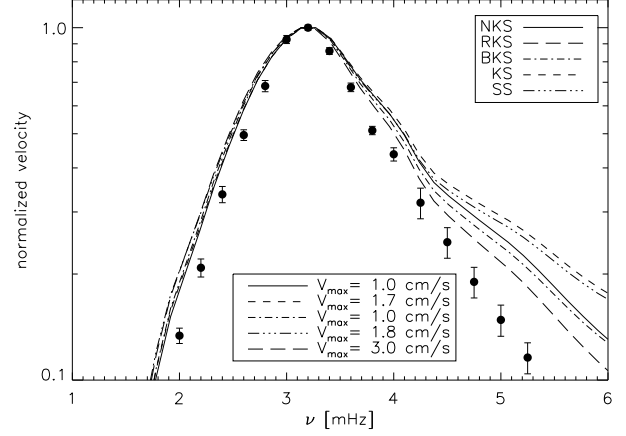


**Fig. 3.** Amplitudes computed with the Reynolds stress contribution only and for the kinetic energy spectra of Fig. 2. A gaussian time spectrum has been adopted. The curves are normalized to their maximum value and have intentionally been shifted by +0.1 mHz in order to match the position of the observed maximum. All other assumptions are those of Fig. 1.

which mimics the solar kinetic spectrum observed by Nesis et al. (1993).

The above five kinetic energy spectra are plotted in Fig. 2. All these spectra exhibit the same  $-5/3$  slope at large wavenumbers. The RKS, the BKS, the SS and the NKS take into account large-scale eddies lying in the injection region.

As stressed by Rieutord et al. (2000), differences at low wavenumber between the kinetic spectra obtained from observations of the solar granulation are a consequence of uncontrolled data-averaging procedures. Properties of the kinetic spectrum at low wavenumber (mesogranulation) are thus not yet well depicted by the observations of the solar surface. In the present paper we nevertheless study the different spectra of Eqs.(11-13) in order to gauge the sensitivity of the acoustic power emission to the properties of the turbulent spectrum in the injection region.

Fig. 3 presents amplitudes computed with the sole Reynolds stress contribution and for the different kinetic energy spectra of Fig. 2. Only small differences in the velocity amplitudes are observed arising from different spectra at low frequencies. The main differences are observed at high frequency where the RKS and BKS exhibit a steeper slope than the KS and SS. These features are explained below.

The velocity amplitudes obtained by B92 using the KS are shifted by a larger amount toward lower frequencies compared to ours and differences between the KS and SS are found to be larger in Houdek (1996), in which computations are based on the formulation of B92. The last feature is due to the way B92 implemented the SS and the first feature is due to the way we normalized the turbulent energy spectra (Eq. 63 in Paper I).

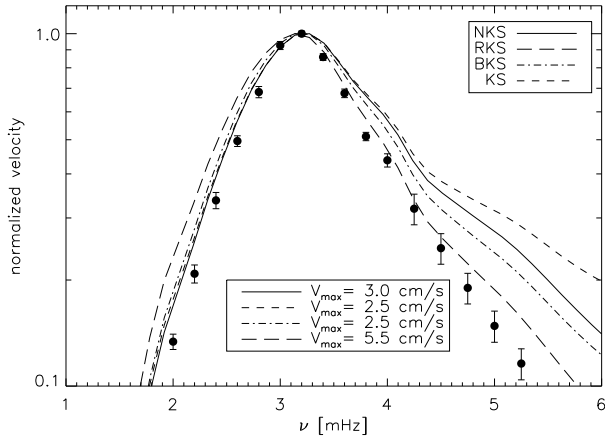


**Fig. 4.** Velocity amplitudes computed with both the Reynolds and the entropy contributions and for different kinetic energy spectra. A gaussian time spectrum has been adopted. The curves are normalized to their maximum value and have intentionally been shifted by +0.1 mHz in order to match the position of the observed maximum. Dots are observational points as defined in Fig.1. The free parameters are set to  $\lambda = 1$ ,  $\beta = 1.9$ .

With our formulation, velocity amplitudes using the SS are similar to those using the KS. Therefore we no longer consider the SS in the remaining part of this work.

From here on, amplitudes calculations include both Reynolds stress and entropy contributions. Fig. 4 shows amplitudes computed with the free parameters set to  $\lambda = 1$ ,  $\beta = 1.9$  with  $\Phi = 2$ . Large differences are found at high frequencies arising from the use of different turbulent spectra. The RKS leads to larger amplitudes and fits better the solar observations at high frequencies. At low frequencies, the RKS overestimates  $v_s$  more than the estimates including only the Reynolds stress contribution. The RKS contains a significant amount of kinetic energy at low wavenumbers. At low frequencies the excitation process is mainly due to the large scale eddies. Furthermore it is stressed in Paper I that the entropy contribution is more efficient for long-period oscillation modes. Therefore the RKS injects through the entropy contribution a larger amount of energy to the low frequency modes than the other spectra. For the other spectra we found few differences in terms of frequency dependence between computations including only the Reynolds stress contribution and including both Reynolds stress and entropy contributions.

The computed  $P_{\omega_0}$  is plotted in Fig. 5 in order to emphasize the changes due to the use of different turbulent spectra. Also shown is the power  $P_{\omega_0}$  derived from the observations according to Eq.(7) where the radius  $r_s$  corresponds to the layer at which  $v_s$  is measured. We observe large differences between the oscillation spectra  $P_{\omega_0}$ . At high frequency, the KS strongly overestimates  $P_{\omega_0}$  while the RKS and the BKS are closer to the oscillation power derived from the observations. Thus the RKS and BKS

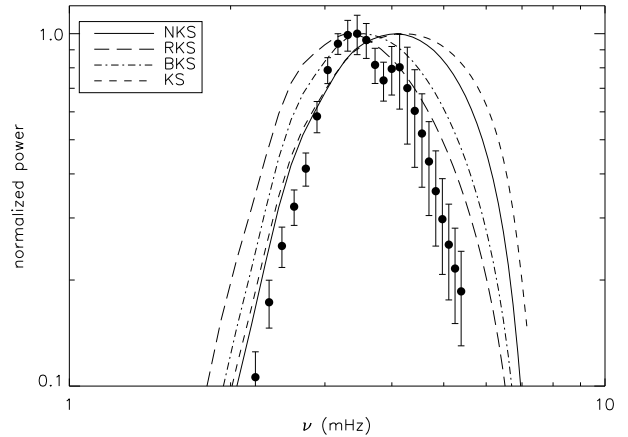


**Fig. 5.**  $P_{\omega_0}$  for different kinetic energy spectra are presented in  $\log - \log$  representation. Dots represent the oscillation power derived from the solar observations with the help of Eq. (7). Corresponding errors bars are plotted.

inject relatively less energy into the high frequency oscillations. This is explained as follows: contributive eddies are those for which  $\tau_k \omega_0 \lesssim 1$ . At a given wavenumber  $k$  the RKS induces a smaller velocity  $u_k$  for the considered eddy. As  $\tau_k \approx (k u_k)^{-1}$  for a given oscillation frequency, the RKS then involves eddies with larger wavenumbers than the KS. Eddies with a high wavenumber carry less energy and consequently the RKS injects relatively less power into the oscillations of high frequencies than the KS does.

At low frequencies smaller differences are observed between the spectra because for small values of the oscillations frequencies all the eddies of the spectra are involved in the excitation process. However, the RKS overestimates  $P_{\omega_0}$  while the BKS leads to an intermediate result between the RKS and the KS.

Fig. 6 compares the sizes of the excitation region when using the KS and the RKS for several oscillation modes. It shows that the depth dependence of  $P(\omega)$  behaves according to the depth dependence of the associated displacement eigenfunction. For higher radial order, the mode is more concentrated toward the surface and consequently the excitation region is shallower. The extension of the excitation region is about twice the size with the KS than with the RKS; i.e.  $\approx 1.5$  Mm with the KS against  $\approx 0.8$  Mm with the RKS and for a mode of order  $n = 20$  and a frequency  $\nu \approx 3$  mHz. This can be explained as follows: For a given wavenumber  $k$ , the correlation time of an eddy, is larger with the RKS than with the KS because the RKS induces smaller velocity  $u_k$  at a given wavenumber  $k$ . Therefore the region where  $\tau_k \omega_0 \lesssim 1$  is smaller with the RKS. This explains the strong differences in terms of depth of excitation found between the KS and the RKS (Fig. 6). The BKS induces an intermediate depth of excitation between the RKS and the KS (not shown here). Therefore the RKS induces a thinner excitation region

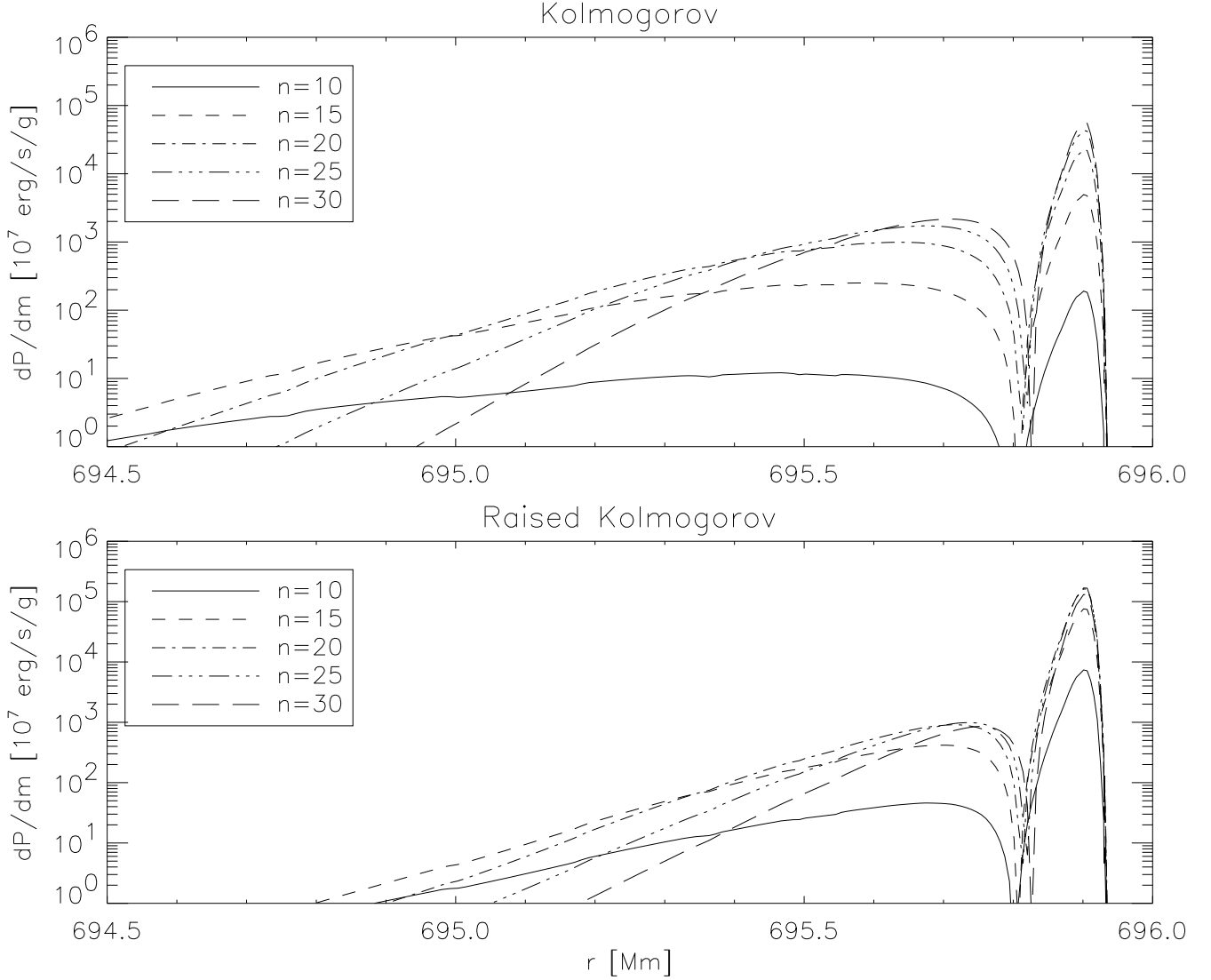


**Fig. 6.** Depth dependence of the injected power in the solar outer layers computed for the oscillation modes of radial order  $n = [10, 15, 20, 25, 30]$ . The abscissae are the stellar radius from center in Mm. The oscillation power is plotted for the KS (top) and the RKS (bottom) with  $\lambda = 1$  and  $\beta = 1.9$ . All other assumptions are the same as in Fig.4.

which is closer to the one found in the simulation performed by Stein & Nordlund (2000).

### 3.2. Turbulent entropy spectrum

It has been assumed above that the entropy spectrum exhibits the same behavior as the kinetic energy spectrum. However, in paper I, we stress that the entropy spectrum exhibits the same behavior as the temperature spectrum and the turbulence theory (Lesieur, 1997, Chap VI-10) predicts a specific spectrum for the turbulent temperature fluctuations which derives from the scalar nature of the temperature. We therefore proposed the “conductive” entropy spectrum derived from the theoretical spectrum

expected for the temperature fluctuations (Lesieur, 1997)

$$E_s(K) = \begin{cases} \frac{a_0 \tilde{s}^2}{u_0^2 k_0} E(K) & \text{for } 1 < K < K_C \\ \frac{a_0 \tilde{s}^2}{u_0^2 k_0} \left(\frac{K_C}{K}\right)^4 E(K) & \text{for } K_C < K \end{cases} \quad (14)$$

where  $a_0$  is a normalization factor,  $E(K)$  is the kinetic energy spectrum,  $\tilde{s}^2$  is the entropy scalar variance (Eq. 88 of Paper I) and  $K_C \equiv k_c/k_0$  where  $k_c$  is the wavenumber which separates the inertial-convective range from the inertial-conductive range. When the kinetic energy spectrum  $E(k)$  obeys the Kolmogorov scaling law, the entropy spectrum verifies

$$E_s(K) = \begin{cases} \frac{a_0 \tilde{s}^2}{k_0} K^{-5/3} & \text{for } 1 < K < K_C \\ \frac{a_0 \tilde{s}^2}{k_0} K_C^4 K^{-17/3} & \text{for } K_C < K \end{cases} \quad (15)$$

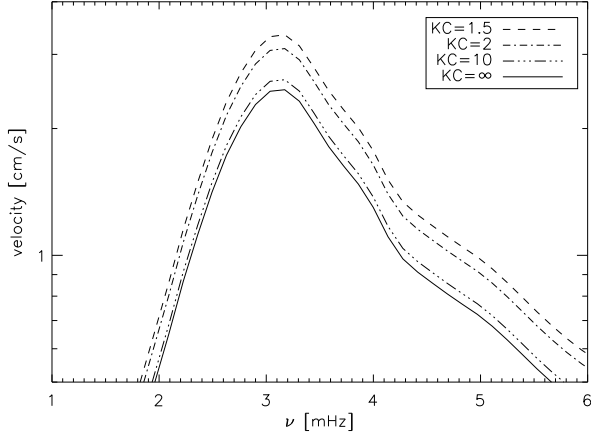


**Fig. 7.** Amplitudes computed with the “Kolmogorov Conductive spectrum” (KCS) for different values of  $K_C$ . All other assumptions are those of Fig.4.

This spectrum, that we call the “Kolmogorov Conductive spectrum” (KCS, hereafter), matches observations of intensity fluctuations of the solar granulation performed by Espagnet et al. (1993) and Nesis et al. (1993).

There is no theoretical constraints on the value of  $K_C$ ; therefore  $K_C$  may be considered as a free parameter of our formulation. We thus investigate different values of  $K_C$  with the use of the KCS (Eq.15). The results are presented in Fig. 7.

We observe no change in the shape when varying  $K_C$ , only a decrease of the global amplitudes with increasing  $K_C$ . As  $K_C$  decreases, the major part of the energy in the entropy energy spectrum is concentrated at low wavenumbers. Eddies with small wavenumbers carry more energy than those with larger wavenumbers. Therefore a decreasing value of  $K_C$  induces an increase of  $P_{\omega_0}$  and thus the shape of  $v_s(\omega_0)$  remains unchanged. We found similar results with the entropy “conductive” spectra based on the RKS, BKS and NKS (not shown here) and derived from Eq.(14).

Therefore we cannot constrain the value of  $K_C$  from the seismic solar observations. However Espagnet et al. (1993) shows that the inertial-convective domain of the temperature spectrum starts from granular scales of about  $k_0 \approx 3 \text{ M}^{-1}\text{m}$  while the inertial-conductive range starts from  $k_c \approx 6 \text{ M}^{-1}\text{m}$ . This leads to a value  $K_C = 2$ .

In the remaining part of this work, the computation of  $P_{\omega_0}$  will be performed assuming the “conductive” spectra for the entropy contribution with  $K_c = 2$ .

### 3.3. Time spectrum

The time spectrum function of eddies with given  $k$  is usually modelled by a gaussian function in which linewidth is proportional to the time correlation of the eddy (Goldreich & Keeley, 1977; Balmforth, 1992, Paper I). As proposed by Stein (1967) and Musielak et al. (1994) we also con-

sider below other forms for the time spectrum  $\chi_k(\omega)$  such as the modified gaussian form

$$\chi_k(\omega) = \frac{2}{\sqrt{\pi}} \frac{\omega^2}{\omega_k^3} e^{-(\omega/\omega_k)^2} \quad (16)$$

and an exponential form

$$\chi_k(\omega) = \frac{1}{2\omega_k} e^{-|\omega/\omega_k|}. \quad (17)$$

The quantity  $\omega_k$  controls the width of the eddy time spectrum and is therefore related to the eddy correlation time as  $\omega_k = 2/\tau_k$  (see Paper I). All time spectra are normalized such that

$$\int_{-\infty}^{+\infty} \chi_k(\omega) d\omega = 1. \quad (18)$$

This choice of normalization differs from the one considered by Musielak et al. (1994), but is in agreement with Tennekes & Lumley (1982) requirements.

Fig. 8 shows the normalized velocity amplitudes  $v_s$  computed with the RKS and for different time spectra : the gaussian form, the modified gaussian and the exponential forms. Both the exponential and the modified gaussian forms yield amplitudes which are too large compared with the observations at high frequencies while the gaussian form gives rise to amplitudes which are closer to the observed amplitudes. At low frequencies both the modified gaussian and the exponential forms fall slightly closer to the observations than the gaussian form. In contrast, computed  $v_s$  assuming the KS leads to the opposite behavior for the gaussian form, *i.e.* at low frequencies, computed  $v_s$  with the gaussian form are closer to the observations than the other forms (not shown here).

The strongest disagreement between observed and computed surface velocity amplitudes using KS and RKS is obtained at high frequency for the exponential form. Therefore we discard this time spectrum from now on. We cannot clearly discriminate between the modified gaussian form and the gaussian form and choose to adopt the gaussian form.

### 3.4. Influence of the atmosphere

We have computed two solar models, one with the Eddington classical gray atmosphere and one with the Kurucz ATLAS 9 (Kurucz, 1991) solar model atmosphere. The differences in the computed powers (not shown here) are found to be much smaller than effects due to the choice of the kinetic spectrum and than the errors in the observations.

On the other hand, the measured velocity amplitudes  $v_s$  depend on the height in the atmosphere where the observations are sampled. Fig. 9 shows theoretical velocity amplitudes calculated at different heights in the atmosphere.

Changes in the eigenfunction profiles at the solar surface are larger with high frequency modes. Therefore increasing the height in the atmosphere where  $v_s$  is computed leads to larger changes at high frequencies ( $\nu \gtrsim$

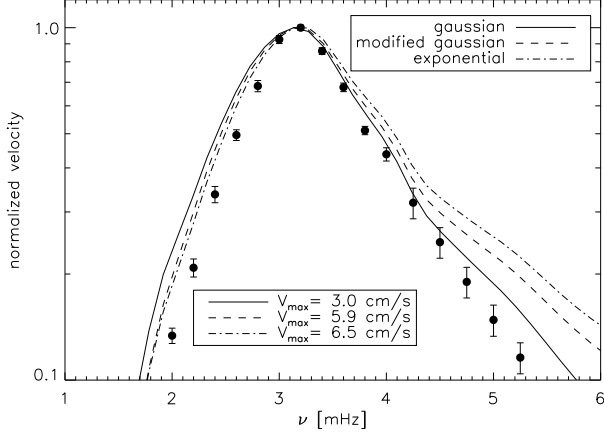


**Fig. 8.** Computed  $v_s(\omega_0)$  assuming the RKS is plotted for different frequency factors  $\chi_k(\omega)$ . All other assumptions are those of Fig. 3

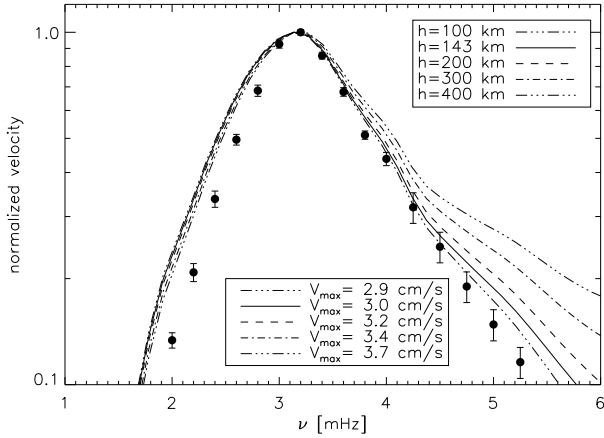


**Fig. 9.** Velocity amplitudes  $v_s$  computed at different levels in the atmosphere and using the RKS. Other assumptions are those of Fig.4.

3.5 mHz). Almost no effect is observed at low frequencies. This shows that the physics of the excitation process is more easily constrained by the observations at low frequencies ( $\nu \lesssim 3.5$  mHz).

### 3.5. Effects of the free parameters $\lambda$ and $\beta$

With  $k_0$  given by Eq.6, the eddy time correlation length (Eq.5) can be related to  $\beta$  and  $\lambda$  as

$$\tau_k = \frac{\lambda \beta}{\omega_\Lambda K u_K} \quad (19)$$

where  $\omega_\Lambda = 2\pi u_0/\Lambda$  and  $u_K = u_k/u_0$ . Thus both  $\beta$  and  $\lambda$  are involved in the expression of the amplitude (Eq. 101, Eq. 102 and Eq. 103 of Paper I). The product  $\beta \lambda$  controls the frequency-dependence of the oscillation power. Fixing the value of  $\beta$  to 1, we investigate the effects of changing

the parameter  $\lambda$ . In terms of frequency dependence, this is equivalent to fixing  $\lambda$  and to varying the parameter  $\beta$ .

Fig. 10 shows velocity amplitudes  $v_s$  computed when assuming the KS, the RKS and the NKS for different values of  $\lambda$ . The value of  $\lambda$  (or  $\beta$ ) controls the extension of the excitation region through  $\tau_k$ . Small values of  $\lambda$  lead to a larger excitation region and therefore favor long-period oscillation modes. This explains the larger frequency shift of the maximum amplitude between the computations and the observations obtained with  $\lambda \lesssim 1$ . Changing  $\lambda$  has smaller effects at low frequencies than at high frequencies because at low frequencies all the eddies in the spectra are involved in the excitation process and the frequency dependence is mainly controlled by the mode inertia and the derivatives of the eigenfunctions. Changes are nevertheless larger when using the RKS than the NKS and the KS.

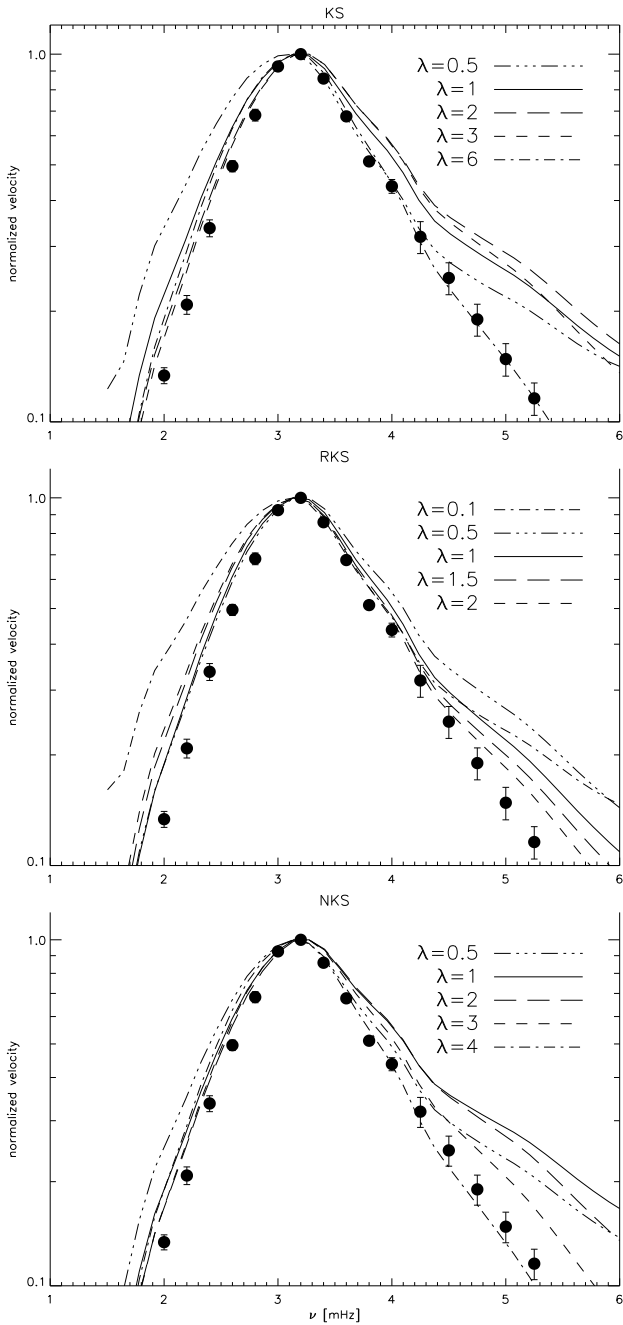
For  $\lambda = 0.5$  and using the KS, the frequency shift between the numerical results and the observations is about 0.25 mHz and the computations overestimate the amplitudes at low frequencies. In that case, the velocity  $v_s(\omega_0)$  is close that found by B92 and Houdek (1996) which assumed  $\lambda = 1$ . This result is consistent with the Osaki (1993) statement that the B92 formulation leads to a source of excitation that is too extended. Our estimates with  $\lambda = 1$  and using the KS are closer to the observations than those performed by B92 and Houdek (1996). This difference is due to the way we have normalized the turbulent energy spectra. Therefore our formulation leads to a smaller depth of excitation and is in better agreement with the observations.

We observe large changes at high frequencies with  $\lambda$  for all the spectra. Increasing  $\lambda$  induces a steeper slope at high frequency. This can be explained as follows: contributive eddies are those for which  $\tau_k \omega_0 \lesssim 1$ . These eddies are the eddies for which  $k \gtrsim k_0(\lambda \beta \omega_0 / K u_K \omega_\Lambda)^{3/2}$ . As  $\lambda$  increases, only eddies with higher wavenumbers  $k$  are involved in the excitation process. Therefore, because eddies with high wavenumbers carry less energy,  $P_{\omega_0}$  is smaller with increasing value of  $\lambda$ .

The oscillation amplitude increases as  $\beta^4$ , hence  $\beta$  plays a major role in the control of the maximum amplitude. A theoretical constraint can be obtained for  $\beta$  as  $\beta \lambda \lesssim 2.7 \Phi^{1/2}$  (see paper I). For  $\Phi = 2$ , we have  $\beta \lambda \lesssim 4$ .

## 4. Solar calibration

We need to determine the free parameters  $\lambda$  and  $\beta$  by calibrating the theoretical amplitudes on the solar observational ones. For each of the various kinetic and “conductive” spectra, we first adjust  $\beta \lambda$  in order to match as closely as possible the position of the maximum and when possible the frequency dependence of  $v_s(\omega_0)$  to the observed surface velocity given by Libbrecht (1988). We next adjust  $\beta$  and  $\lambda$  in such a way as to obtain the observed maximum value of  $18 \text{ cm s}^{-1}$ . Table 1 gives the values of the adjusted parameters.



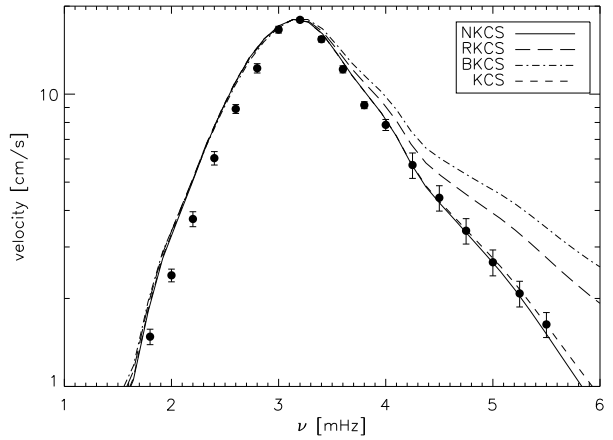
**Fig. 10.** Surface velocity  $v_s(\omega_0)$  computed with  $\beta = 1$  for different values of the parameter  $\lambda$ . The top panel concerns the KS, the middle one the RKS and the bottom one the NKS. All other assumptions are those of Fig. 4.

Fig. 11 shows amplitudes computed with the RKS, KS, BKS and NKS with  $\beta$  and  $\lambda$  set to their adjusted values. The KS and NKS yield much better fits to the seismic observations than the other spectra.

Observations of solar granulation by Espagnet et al. (1993) show that  $k_0 \simeq 3 \text{ Mm}^{-1}$  whereas a value of  $k_0 \simeq 7 \text{ Mm}^{-1}$  can be inferred from the observations of Nesis et al. (1993). These values correspond to  $\beta \approx 8$  and  $\beta \approx 4$  respectively. The values of  $\beta$  adjusted with the RKS, the BKS and the NKS are closer to the value of  $\beta$  suggested

**Table 1.** Values of the adjusted parameters  $\beta$  and  $\lambda$ . The wavenumbers  $k_0$  of the largest eddies in the inertial range have been evaluated at the solar radius according to the relation  $k_0 = 2\pi/\beta\Lambda$ . We have assumed the “conductive” spectra and  $K_C = 2$ .

spectrum	$\beta\lambda$	$\beta$	$\lambda$	$k_0 (\text{Mm}^{-1})$
RKS	1	3.53	0.28	7.3
BKS	1	4.44	0.22	5.8
NKS	3.8	5.00	0.76	5.1
KS	5.7	9.51	0.60	2.7



**Fig. 11.** Velocity amplitudes computed with the RKS, BKS, NKS and KS with values of the parameters  $\beta$  and  $\lambda$  as given in Table 1. All other assumptions are those of Fig. 4.

by the observations of Nesis et al. (1993) while the value suggested by the observations of Espagnet et al. (1993) favors the KS. Therefore  $\beta$  is not well constrained by the observations of the solar granulation and this cannot help to discriminate between the different turbulent spectra.

The best fits are obtained with the NKS and the KS. The power computed with the KS seems to fit best the observations; this can be explained by the existence of compensating effects. We indeed know from the observations of the solar granulation that kinetic energy is carried by large-scale eddies. This corresponds to the  $k$ -injection region lying at scales above the inertial range, which is not described by KS. Furthermore, the theoretical constraint imposed on  $\beta\lambda$  (see Sect. 3.5) suggests that the adjustment value of  $\beta\lambda$  found by fitting the amplitudes with the KS to the observations is not valid, while the other spectra verify this constraint. One is therefore left with the NKS,  $\lambda = 0.76$  and  $\beta = 5.0$  as our best fit of the solar data. However, the fit is not perfect at low frequencies. We show in Samadi et al. (2001) that this is related to the treatment of the static model and the corresponding oscillations.

## 5. Conclusion

Acoustic power and oscillation amplitudes of radial oscillations computed for a solar model are compared with solar seismic observations. With the adopted approach for computing the acoustic power (paper I), we find that the entropy source term significantly contributes to the excitation process of solar-like oscillations by turbulent convection, in agreement with the results of GMK and simulations by Stein & Nordlund (1991).

Our generalized formulation for the oscillations power  $P_{\omega_0}$  injected into the modes allows us to investigate effects of changes in the turbulent components.

In the solar case, several kinetic energy spectra have been considered: the Kolmogorov spectrum (KS); the “Raised Kolmogorov Spectrum” (RKS) which is derived from observations of the solar granulation by Roudier & Muller (1986); the “Nesis Kolmogorov Spectrum” (NKS) which is derived from observations performed by Nesis et al. (1993). We have, in addition, considered the “Spiegel Spectrum” (SS) which takes into account the non-linear interaction between turbulent modes of low wavenumber and the “Broad Kolmogorov Spectrum” (BKS) which exhibits intermediate properties between the SS and the NKS at low wavenumbers.

In a first step, the value of the free parameter  $\beta$  is set to a value loosely determined using theoretical arguments and  $\lambda = 1$  is assumed as in B92. The oscillation power spectra computed with the KS, BKS, NKS and RKS significantly differ. In contrast with Houdek’s (1996) results, only small differences between the KS and SS are found. At high frequency, the RKS gives rise to a frequency dependence of the velocity which more closely fits the frequency dependence of the solar observations than the other spectra and in addition induces larger amplitudes. Moreover, the RKS leads to a depth of excitation of the same order as the one found by Stein & Nordlund (2000). This depth of excitation is found to be much smaller than the one associated with the KS. This result is in agreement with Osaki’s (1993) statement that the source of excitation should be more concentrated than the extended source distribution found by B92.

As a model for the time spectrum of the turbulent eddies, we find that the gaussian form, which is usually considered, and the modified gaussian proposed by Musielak et al. (1994), both agree with the observations while the exponential form - also proposed by Musielak et al. (1994) - is not satisfactory.

We have assumed an entropy spectrum which is expected from the turbulent theory. This spectrum presents a steeper slope in the inertial-conductive region, i.e. above the wavenumber  $k_c$ . Only changes in the global amplitudes are observed when changing  $k_c$ : the amplitude increases with decreasing values of  $k_c$ . Thus the value of  $k_c$  is difficult to constrain because the global amplitude depends on the treatment of convection. Therefore the entropy spectrum expected from the theory cannot be validated with the solar seismic observations. The value of  $k_c$  has thus

been set to the value suggested by the observations of the solar granulation by Espagnet et al. (1993).

Assuming a theoretical value for the free parameter  $\beta$  (as suggested in Paper I) for each spectrum, we find that the absolute amplitude remains much smaller than the observations (about 3 – 5 cm/s). Because the formulation is very sensitive to  $\beta$ , the observed differences in the maximum amplitude between the theoretical estimates and the observations are mainly related to the uncertainties in the determination of  $\beta$ . Observations of solar granulation are not accurate enough to provide a very precise value of the parameter  $\beta$ . Also the product  $\beta\lambda$  controls the depth of excitation and therefore also the frequency dependence of the expected power. Accordingly,  $\beta\lambda$  is given a value for each spectrum which best matches the frequency dependence of the power spectrum at low frequencies to the observations. We next determine the value of  $\beta$  and  $\lambda$  in order to adjust the maximum amplitude to the observations. This in turn defines the eddy time correlation and the scale at which energy injection is initiated.

Doing so, all the turbulent spectra give rise to a similar behavior for  $P_{\omega_0}$  at low frequencies but the KS and NKS fit much better the observations at high frequencies. The values of  $\beta$  and  $\lambda$  resulting from the fitting performed with the RKS, BKS and NKS are found to be compatible with the Nesis et al. (1993) observations of the solar granulation. For the KS we find much larger values of  $\beta$  and  $\lambda$ . The corresponding value of  $\beta\lambda$  is not compatible with the estimated upper limit value of  $\beta\lambda$ . This suggests that the NKS is in better agreement with the observed surface velocity spectrum of the Sun

The agreement in using the NKS between theoretical results and solar observations is found to be much better than that obtained in previous work. In particular at high frequencies, the power derived from the observations exhibits a slope of about  $-6$  above  $\nu = 4.5$  mHz.

GMK predicts a slope of about  $-4.4$  and a slope of about  $-1.0$  is found with B92’s formulation. In the present work, we find a slope  $\log(P_{\omega_0})$  vs  $\log(\nu)$  of about  $-6$  in the frequency domain  $\nu \gtrsim 4.5$  mHz.

It is not obvious that the above conclusions hold true for other solar-like oscillating stars. In particular one expects  $P_{\omega_0}$  to exhibit different properties for stars with rotation and magnetic activity which are different to that of the Sun and the NKS might well not be suitable to represent the actual turbulent spectrum in these stars.

Assuming the same properties of turbulence i.e. same values of the free parameters for a given turbulent spectrum, it is possible to apply our calibrated formulation to several potentially solar-like oscillating stars in order to investigate the consequences of changing the turbulent ingredients and to establish constraints on the stellar turbulent spectrum (Samadi et al., 2000, 2001).

On the theoretical side, further tests and validation are needed. In particular, as suggested in Paper I, 3D simulations of the stellar convection will enable us to test some of the assumptions and approximations entering the present formulation (Samadi, 2000). In addition, such simulations

may enable us to constrain more accurately the values of the free parameters than has been achieved here with solar seismic data.

*Acknowledgements.* We thank F. Tran Minh and L. Leon for the use of the FILOU pulsation code and we are indebted to J.-P. Zahn for useful discussions.

## References

- Baglin, A. & The Corot Team. 1998, in IAU Symp. 185: New Eyes to See Inside the Sun and Stars, Vol. 185, 301
- Balmforth, N. J. 1992, MNRAS, 255, 639
- Böhm - Vitense, E. 1958, Zeitschr. Astrophys., 46, 108
- Espagnet, O., Muller, R., Roudier, T., & Mein, N. 1993, A&A, 271, 589
- Goldreich, P. & Keeley, D. A. 1977, ApJ, 212, 243
- Goldreich, P. & Kumar, P. 1990, ApJ, 363, 694
- Goldreich, P., Murray, N., & Kumar, P. 1994, ApJ, 424, 466
- Grevesse, N. & Noels, A. 1993, in Origin and Evolution of the Elements, ed. N. Prantzos, E. Vangioni-Flam, & M. Cassé (Cambridge University Press)
- Houdek, G. 1996, PhD thesis, Institut für Astronomie , Wien
- Kjeldsen, H. & Bedding, T., eds. 1998, The First MONS Workshop: Science with a Small Space Telescope, ed. H. Kjeldsen & T. Bedding, Aarhus Universitet.
- Kurucz, R. L. 1991, in Stellar Atmospheres - Beyond Classical Models, 441
- Lebreton, Y., Perrin, M., Cayrel, R., Baglin, A., & Fernandes, J. 1999, A&A, 350, 587
- Lesieur, M. 1997, Turbulence in fluids (Kluwer Academic Publishers)
- Libbrecht, K. G. 1988, ApJ, 334, 510
- Matthews, J. M. 1998, in Structure and Dynamics of the Interior of the Sun and Sun-like Stars, 395
- Morel, P. 1997, A&AS, 124, 597
- Musielak, Z. E., Rosner, R., Stein, R. F., & Ulmschneider, P. 1994, ApJ, 423, 474
- Nesis, A., Hanslmeier, A., Hammer, R., Komm, R., Mattig, W., & Staiger, J. 1993, A&A, 279, 599
- Osaki, Y. 1993, in ASP Conf. Ser. 40: IAU Colloq. 137: Inside the Stars, 512-520
- Rieutord, M., Roudier, T., Malherbe, J. M., & Rincon, F. 2000, A&A, 357, 1063
- Roudier, T. & Muller, R. 1986, Solar Phys., 107, 11
- Samadi, R. 2000, PhD thesis, Université Paris 6
- Samadi, R. & Goupil, M.-J. 2001, A&A(in press)
- Samadi, R., Goupil, M.-J., Lebreton, Y., & Baglin, A. 2000, in SOHO 10 / GONG 2000 Workshop (in press)
- Samadi, R., Houdek, G., Goupil, M.-J., & Lebreton, Y. 2001, submitted to A&A
- Spiegel, E. 1962, J. Geophys. Res., 67, 3063
- Stein, F. & Nordlund, A. 1991, in Challenges to Theories of the Structure of Moderate-Mass Stars, Vol. 195 (ed D. Gough & J. Toomre (Springer-Verlag))
- Stein, R. F. 1967, Solar Physics, 2, 385
- Stein, R. F. & Nordlund, A. 2000, ApJ(in press)
- Tennekes, H. & Lumley, J. 1982, A first course in turbulence, 8<sup>th</sup> edn. (MIT Press)
- Tran Minh, F. & Leon, L. 1995, in Physical Process in Astrophysics, 219